Optimization of the Solid-Rocket Assisted Space Shuttle Ascent Trajectory

Ivan L. Johnson*
NASA Lyndon B. Johnson Space Center, Houston, Tex.

Optimal solid-rocket assisted space shuttle ascent trajectories are investigated. Solid-rocket thrust profiles are simulated by using third-degree spline functions, with the values of the thrust ordinates defined as parameters. The trajectories are optimized parametrically—with use of the Davidon-Fletcher-Powell, penalty function method—by minimizing propellant weight subject to state and control inequality constraints and terminal boundary conditions. This study shows that optimizing a control variable parametrically by using third-degree-spline-function interpolation allows the control to be shaped so that inequality constraints are strictly adhered to and all corners are eliminated. The absence of corners makes this method attractive from the viewpoint of solid-rocket grain design limitations.

Nomenclature

a_a = axial acceleration
a_{ji} = spline function coefficients
b_i = coefficients for cubic polynomial during tailoff
C_n = aerodynamic normal force coefficient
D = drag force
e $= e_1 + e_2 + \ldots + e_i$
e_i = error functions
g_i = ith point equality constraint
g_0 = gravitational constant
h_i = ith point inequality constraint
I_{sp} = specific impulse
k_j = weight constants or penalty constants for point equality constraints
ℓ_j = weight constants or penalty constants for point inequality constraints
m = mass
n_g = number of point equality constraints
n_h = number of point inequality constraints
Q = dynamic pressure
s_i = state and control inequality constraints
T = thrust magnitude
t = time
t_f = final time
t_0 = initial time
U = unit step function
v = magnitude of relative velocity
W_p = propellant weight
y = nondimensional time variable $(t - t_{\text{tail}}) / \Delta t_T$
z = nondimensional time variable $(t - t_i) / (t_{i+1} - t_i)$
α = angle of attack
ρ = atmospheric density

Subscripts

i = ith value
max = maximum
min = minimum
spln = spline curve fit of
stage = evaluated at staging
steer = evaluated at time when optimal steering begins
tail = during tailoff

Superscripts

($\dot{}$) = d/dt

Presented as Paper 74-823 at the AIAA Mechanics and Control of Flight Conference, Anaheim, Calif., August 5-9, 1974; submitted August 19, 1974; revision received June 4, 1975.

Index category: Spacecraft Attitude Dynamics and Control.

*Aerospace Technologist, Mission Planning and Analysis Division.

Introduction

A major contribution to the cost per flight of a shuttle-type vehicle is the cost of the solid-rocket boosters (SRB's), which assist the orbiter in inserting a specified payload. An important element of the total SRB cost is the cost incurred by the weight of propellant, approximately \$1.20/lb/flight. Sometimes a significant reduction in SRB propellant weight, and therefore cost, may be realized, even with due regard to the constraints imposed on the flight, by optimally shaping the SRB thrust profile.

Previous SRB-assisted space shuttle ascents were shaped optimally by assuming that thrust (vacuum) could be simulated by a sequence of piecewise continuous linear segments, with the values of thrust (vacuum) at each junction point treated as parameters.[1,2] This type of modeling or interpolation presents several inefficiencies and problems. The corners formed at the juncture points within the sequence of piecewise linear segments in a feasible thrust profile represent discontinuities in derivatives of thrust. These discontinuities are undesirable to an engineer trying to determine an actual SRB thrust profile to simulate the sequence of linear segments. Moreover, the linear-segments approach constrains the thrust between data points to a straight line; this prevents, with respect to optimally reducing SRB propellant weight, efficient handling of state and control inequality constraints on dynamic pressure and axial acceleration.

In Refs. 1 and 2 and in the shuttle contractor's solution, the maximum dynamic pressure inequality constraint $\rho v^2/2 \leq 650$ psf was satisfied in terms of dynamic pressure passage through 650 psf at only one instant. This is because the constraint was approximated as a point inequality constraint at the instant dynamic pressure reached its maximum and because of thrust rate limitations.

References 1 and 2 and the contractor treatment did not contend with the axial acceleration constraint $a_a \leq 3g_0$. However, use of a single straight line for thrust during this time results in only a small loss in performance.

Thrust profiles of sectionally linear design lose considerable performance in terms of SRB propellant weight. On the other hand, a variationally optimal solution would yield a thrust-time curve that, after encountering a constraint boundary, might ride it until some other constraint is met. This is difficult to approximate if piecewise continuous linear segments are used for thrust modeling unless a very large number of segments is chosen. Still, corners would probably remain a problem, and the number of parameters required may be quite large. Kelley and Denham[3] explain that the use of cubic spline functions for modeling may offer an attractive compromise between number of parameters (resulting from use of many segments) and overall smoothness of the resulting control. In addition, because of the nature of this sequence of third-degree polynomials interpolating thrust, entry to and exit from inequality constraint boundaries will tend to be smooth.

This report presents the results of a study that employed third-degree-spline-function (cubic-spline-function) interpolation[4] to reduce SRB propellant weight by parametrically optimizing an SRB-assisted ascent trajectory. The parameter optimization method used is the Davidon-Fletcher-Powell, penalty function method.[5-7] Also used was an error function method[8] that efficiently satisfies inequality constraints on dynamic pressure and axial acceleration and design constraints on maximum thrust and thrust rate.

For this study, the shuttle contractor 1973 solid-rocket thrust profile[9] was chosen for comparison purposes. It is emphasized that the purpose of this paper is to present a mathematical technique for optimizing solid-rocket-assisted ascent trajectories; the paper is not meant to offer a comparison to the present shuttle configuration.

Reference Trajectory

To study reductions in SRB propellant weight, a reference trajectory was generated by solving a maximum payload problem. The data points for the thrust profile were taken from Ref. 9 and interpolated by using third-degree spline functions. The resulting curve is shown in Fig. 1(a). Engine characteristics, weight properties, and a description of the reference trajectory were also taken from Ref. 9. After the maximum payload was found the payload was held constant and the thrust data points were allowed to vary as parameters to reduce SRB propellant.

The reference trajectory used in the study satisfied once-around-abort conditions for the polar mission.[9] The steering after the pitchover until staging is $C_n = 0$ (aerodynamic normal force coefficient). After staging, the steering is a parametrically defined sequence of linear segments.[7,13,14] The following point constraints were defined at insertion

g_1 : altitude = 50 naut miles (1a)

g_2 : velocity = 25,920 fps (1b)

g_3 : flight-path angle = 0.54313° (1c)

g_4 : angle of inclination = 90° (1d)

h_1 : amount of OMS propellant burned ≤ 11,904 lb (1e)

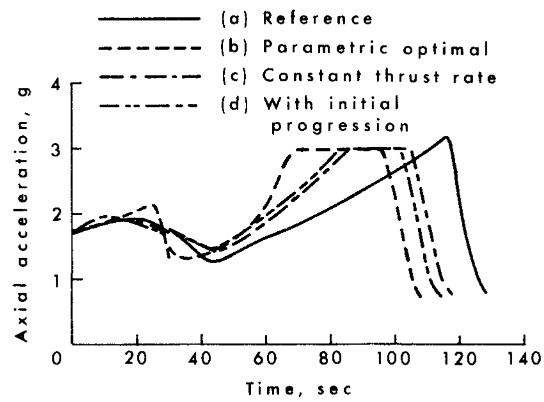

Fig. 3 Axial acceleration vs time.

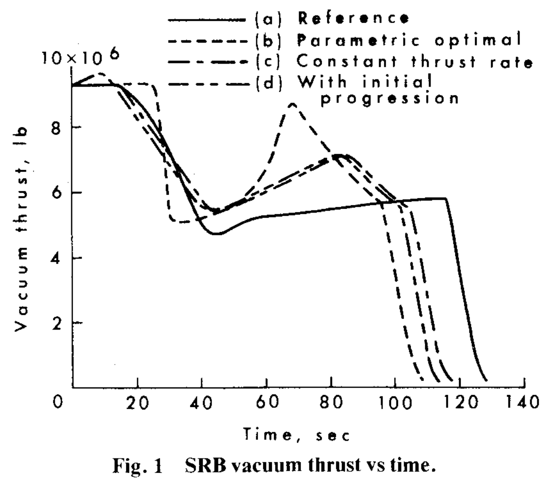

Fig. 1 SRB vacuum thrust vs time.

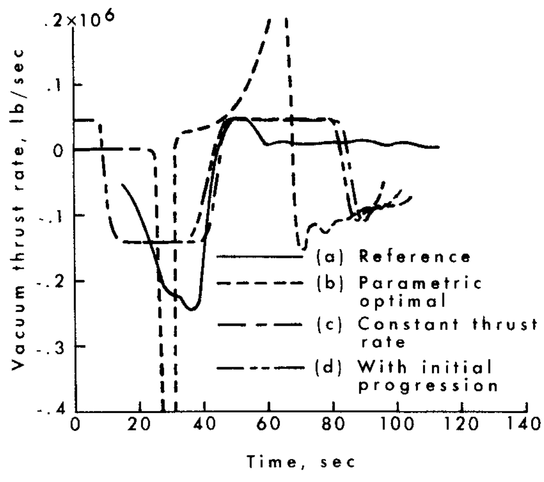

Fig. 4 Vacuum thrust rate vs time.

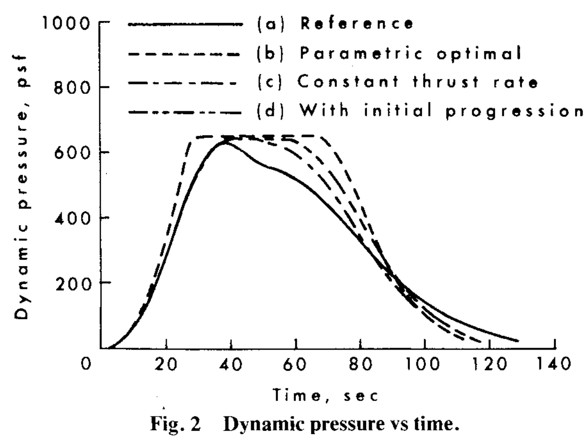

Fig. 2 Dynamic pressure vs time.

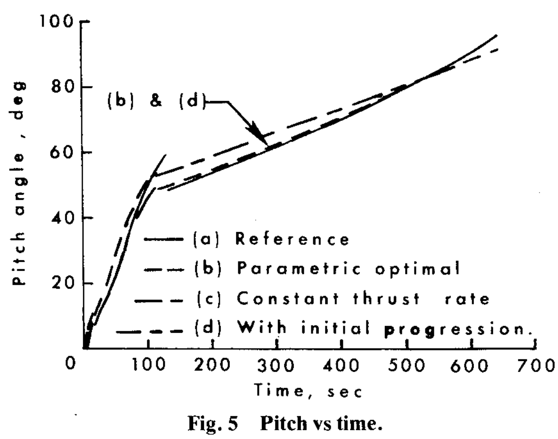

Fig. 5 Pitch vs time.

The maximum payload problem solved produced a maximum payload value of 39,418 lb, compared to 39,256 lb obtained in Ref. 9. Dynamic pressure, axial acceleration, thrust rate, and pitch angle profile are featured in Figs.2(a), 3(a), 4(a), and 5(a). The amount of SRB propellant burned was 2,829,449 lb.

Optimal Thrust Profile

A typical optimal thrust profile for this configuration is depicted in Fig. 6 (a). It consists of a maximum thrust until $Q=\rho v^2/2$ reaches 650 psf at $t=t_1$, then an instantaneous decrease to a level corresponding to $\dot{Q}=0$. Figure 6(b) shows the corresponding changes in the Q curve. From t_1 to t_2, whereas $Q=650$ psf, the thrust is computed from $\dot{Q}=0$. The reason for this is that $Q\leq 650$ psf is a first-order-state-variable inequality constraint.[10] The control thrust, does not appear explicitly in $Q=\rho v^2/2$ but appears in its first derivative in the $\dot{v}$ term

$$\dot{Q}=\rho v\dot{v}+\dot{\rho}v^2/2=0 \tag{2}$$

The equation for this throttle was derived for a similar situation in Ref. 11. From Fig. 6(c), at time t_2, the axial acceleration reaches $3g_0$ before the thrust can rise back to the maximum level. At that point, the thrust will begin to decrease as it rides the axial acceleration constraint boundary

$$(T\cos\alpha-D)/m=3g_0 \tag{3}$$

until $t=t_3$, where tailoff beings. The times $t_1\rightarrow t_3$ would have to be determined by satisfying all of the necessary conditions for an extremum.

For a solid-rocket booster, the optimal thrust profile of Fig. 6(a) suggests the use of two different sets rather than a single set of solid-rocket boosters. Both sets of rockets would burn in parallel until time t_1, at which time one set, having a constant thrust of $(T_{\max}-T^*)$, upon being spent, would be dropped, whereas the other set, having an initial constant thrust T^*, would continue to burn.

Thrust Profile Optimization with Third-Degree-Spline-Function Representation

In the design of a solid-rocket engine, a thrust-time curve and an envelope limitation are furnished.[12] Other factors, such as temperature storage requirements and vehicle overall requirements, are also involved in the selection of a propellant. The total impulse and propellant weight of the desired engine is determined as a function of the thrust-time curve. On the basis of total impulse, propellant weight, and parameters such as chamber pressure, burning rate, surface area, and nozzle throat area, the desired solid-rocket engine can be described.

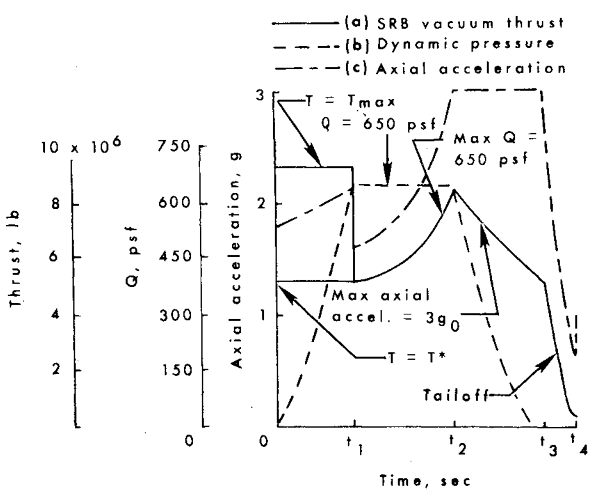

Fig. 6 Optimal solution.

The thrust-time curve, an important influence on the amount of propellant required, if selected efficiently (optimally), can save a significant amount of propellant weight and thereby reduce cost. A comparison of Figs. 1(a) and 6(a) reveals that the reference thrust profile is far from optimal.

Problem Definition

The payload was specified as 39,418 lb, the amount obtained for the reference trajectory. The value of thrust in each data point except the first one (21 points for this case), and the values of the first derivatives at the beginning and end of the spline interpolation interval of thrust vs time, were treated as parameters. The second derivatives could have been specified instead of the first; however, the thrust-time curve shaping is much more sensitive to changes in the first derivatives than it is to changes in the second derivatives. The length of the burn time from $t=30$ sec to thrust tailoff initiation and the time that the optimal steering was begun were also treated as parameters. This brought the total number of parameters to 33, including the ones defined in the reference case. In addition to the constraints defined by Eq. (1), the following constraints were imposed to keep the optimal steering from beginning too early.

$$h_2:\quad Q\leq 25\text{psf} \tag{4a}$$

$$h_3:\quad t_{\text{stage}}\leq t_{\text{steer}} \tag{4b}$$

A measure of performance was defined as the weight of SRB propellant W_p. The problem then was to find the parameters described that locally minimize W_p while satisfying the constraints of Eqs. (1) and (4) and the inequality constraints on dynamic pressure, axial acceleration, and maximum thrust.

Parametric Thrust Profile Modeling

For the SRB propellant weight

$$W_p=(10^6/I_{\text{sp}})\int_0^{t_{\text{stage}}}T(t)\,dt \tag{5}$$

where

$$T(t)=\begin{cases}T_{\max}, & 0\leq t\leq 15 & \text{(6a)}\\ T_{\text{spln}}, & 15<t\leq t_{\text{tail}} & \text{(6b)}\\ T_{\text{tail}}, & t_{\text{tail}}\leq t\leq t_{\text{stage}} & \text{(6c)}\end{cases}$$

Thrust during the time of the spline interpolation T_{spln} between the two data points $[t_i,\ T(t_i)]$ and $[t_{i+1},\ T(t_{i+1})]$, $t_i\leq t\leq t_{i+1}$, is defined by

$$T_{\text{spln}}(t)=T(t_i)+a_{1i}z+a_{2i}z^2+a_{3i}z^3 \tag{7}$$

where $z\equiv(t-t_i)/(t_{i+1}-t_i)$, $t_1=15$, $t_2=20$, $t_3=25$, $t_4=30$, and $t_{i+1}=t_i+(t_{\text{tail}}-30)/18$, $i=4,\ldots,\ 21$. The coefficients a_{1i}, a_{2i}, and a_{3i} are determined by a set of equations based on the use of a third-degree natural spline function for interpolation[4] Also required in the spline interpolation are the slopes $\dot{T}(t_1)$ and $\dot{T}(t_{22})$. During tailoff, the thrust, T_{tail}, is also defined by a cubic

$$T_{\text{tail}}(t)=T(t_{22})+b_1y+b_2y^2+b_3y^3 \tag{8}$$

where

$$y=(t-t_{\text{tail}})/\Delta t_T \tag{9a}$$

$$\Delta t_T\equiv t_{\text{stage}}-t_{\text{tail}} \tag{9b}$$

Initially, without having been shaped, a thrust-time curve modeled with Eqs. (6)-(9) could look like the one shown in Fig. 7. Then

$$W_p = (10^6/I_{sp})\left\{ \sum_{i=1}^{21} \left[T(t_i) + \frac{a_{1i}}{2} + \frac{a_{2i}}{3} + \frac{a_{3i}}{4}\right](t_{i+1}-t_i) + \left[T(22) + \frac{b_1}{2} + \frac{b_2}{3} + \frac{b_3}{4}\right]\Delta t_T + T_{max}15\right\} \qquad (10)$$

Error Function Models

Since the state and control inequality constraints

$$s_1 = \rho v^2/2 - 650 \text{ psf} \leq 0 \qquad (11a)$$

$$s_2 = T(t) - T_{max} \leq 0 \qquad (11b)$$

$$s_3 = (T\cos\alpha - D)/m - 3g_0 \leq 0 \qquad (11c)$$

must be maintained during this time, error functions e_1, e_2, and e_3 are defined.[8,14] An error function of the form

$$e = e_1 + e_2 + e_3 \qquad (12)$$

is accumulated and added to the penalty function.[6]

$$p = W_p + \tfrac{1}{2}\sum_{j=1}^{n_g} k_j g_j^2 + \tfrac{1}{2}\sum_{j=1}^{n_h} \ell_j h_j^2\, U(h_j) + e \qquad (13)$$

The solution for the problem previously described yielded the SRB thrust, dynamic pressure, axial acceleration, thrust rate, and pitch control profiles depicted in Figs. 1(b), 2(b), 3(b), 4(b), and 5(b). The amount of SRB propellant required was reduced by 161,776 lb. A comparison of Figs. 6(a) and 1(b) shows that this solution looks very much like the optimal solution, except that the corners of the thrust profile were rounded off when constraint boundaries were intersected. The corners were rounded as little as the curve fit would permit.

Observation of these two figures and of Fig. 2(b) indicates that the discontinuity in vacuum thrust apparently tended to occur very near $t=30$ sec which corresponds to t_1 in Fig. 6, to throttle down for the $Q=650$ psf dynamic pressure constraint boundary. At $t=30$ sec, the abort solid-rocket engines are dropped, with a resultant instantaneous increase in acceleration due to the instantaneous decrease in weight. Without a method to cut back thrust just before this drop in mass, an instantaneous drop in thrust apparently should be allowed to occur. This can be done mathematically, although the resulting thrust-time curve probably would not be physically feasible. The solution obtained satisfies the conditions without an instantaneous decrease in thrust. Current configurations are not carrying abort solid-rocket engines, so this problem no longer exists.

A comparison of thrust profiles [Figs. 1(a) and 1(b)] reveals that the burn time was shortened by 20.1 sec a result which, besides reducing propellant, also stages the 423,266-lb SRB cases earlier. The pitch profiles [Figs. 5(a) and 5(b)] indicate that the time of optimal steering initiation was reduced by 14.5 sec and the value of the pitch was higher than the reference pitch, a result indicating that the vehicle was flying closer to the local horizontal to reduce gravity losses.[13]

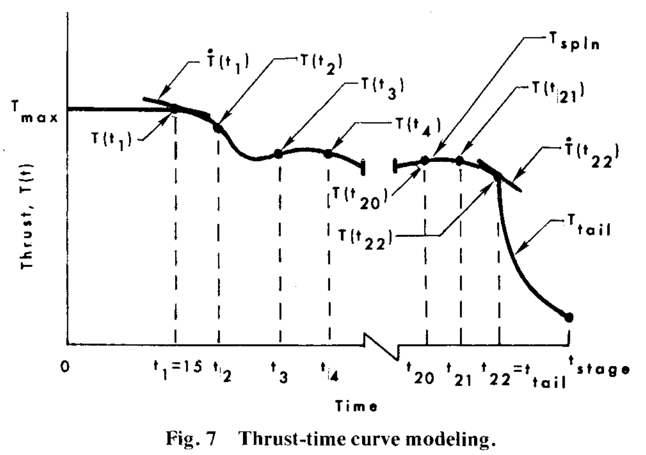

Fig. 7 Thrust-time curve modeling.

Thrust-Rate-Limited Optimal Solutions

Apparently, in the design of a solid rocket engine, one condition that must be satisfied by a thrust-time curve is a restriction on thrust rate at any instant in time. The optimal thrust-time curve in Fig. 1(b) is not a feasible curve by which to design a solid rocket engine because of the large thrust rate magnitudes associated with it. Therefore, another inequality constraint is introduced to constrain the slope of the thrust-time curve during the main burn (the spline interpolation)

$$\dot{T}_{min}(t) \leq \dot{T}(t) \leq \dot{T}_{max}(t) \qquad (14)$$

Since this constraint will be maintained by means of a penalty function, another error function e_4 is defined and added to e in Eq. (12).[8,14] The value of $\dot{T}$ is obtained by evaluating the derivative of Eq. (7). The bounds for $\dot{T}_{min}$ and $\dot{T}_{max}$ are

$$\dot{T}_{min}(t) = -1.5\% \text{ of } T_{max}/\text{sec} \qquad (15a)$$

$$\dot{T}_{max}(t) = 0.5\% \text{ of } T_{max}/\text{sec} \qquad (15b)$$

For this case, the reduction in W_p was 56,088 lb, representing a loss of 65% in the reduction obtained by the optimal thrust-time curve. Figs. 1(c), 2(c), 3(c), 4(c), and 5(c) feature thrust, dynamic pressure, axial acceleration, thrust rate, and pitch for this case.

With an addition of five more data points (parameters) to the spline curve fit and a beginning of interpolation at $t=0$ rather than at $t=15$ seconds, another case was run that also satisfied the constraints (Eq. 15). The reduction in propellant weight was 118,572 pounds. Figures 1(d), 2(d), 3(d), 4(d), and 5(d) feature thrust, dynamic pressure, axial acceleration, thrust rate, and pitch for this case.

Examination of Fig. 1(d) shows that the thrust increased (progressed) initially along the maximum rate boundary. Comparison with Fig. 1(c) shows that the effect of allowing thrust initially to progress shortened the thrust duration by 3 sec and started the throttling down for maximum dynamic pressure about 2 sec earlier.

Discussion of Results

Several points can be observed by studying all of the thrust profiles in Fig. 1. In throttling to meet the maximum-Q constraint, the reference case Fig. 1(a) obviously violates the thrust-rate constraint, [Eq. (15)] and appears more like 1(b) than Fig. 1(c). Also, after observing 3(a), it can be seen that profile 1(a) in Fig. 1 makes no attempt to satisfy the maximum-axial-acceleration constraint [Eq. (3)].

Figure 2, featuring the dynamic pressure curves, reveals several interesting things. First, curve a, the reference curve, did not reach the maximum-Q level (650 psf) but instead reached 630 psf, with a resultant loss of performance. Curve b in Fig. 2 resembles b in Fig. 6, the optimal, very much except for the rounding of the corners where the boundary is encountered. Curves d and c in Fig. 2 resemble each other in that they peak at maximum Q rather than ride the maximum-Q boundary. This is because of the thrust-rate constraints. The dynamic pressure in Fig. 2(d) is shown to be higher at almost all instants and approximates the optimal Fig. 2(b) by becoming a flatter curve near $Q=650$ psf. At t_{stage} for the constant-rate case, Q was below 25 psf and $t_{steer}=t_{stage}$. For curves b and d in Fig. 2, however, $Q=25$ psf was reached 6 sec and 3.5 sec after t_{stage}, respectively.

The axial acceleration and thrust-rate curves (Figs. 3 and 4) are self-explanatory, showing the large thrust-rate magnitudes as expected in Fig. 4(b). The pitch profiles in Fig. 5 exhibit an interesting property. The reference curve a and curve d in Fig. 5 show the pitch profiles decreasing after staging, whereas for the constant-thrust-rate case c, the pitch profile increased. Comparison of b and c in Fig. 5 shows that for b the pitch was much higher, especially after pitchover. This indicates, with reference to Fig. 2, that the vehicle rose, pitched over more, and flew closer to the local horizontal and then throttled earlier to meet the Q constraint.

Conclusions

The results in this study show that the method of third-degree-spline-function interpolation of the control (thrust in this case), connected with the error function technique, is a reasonable way of handling state and control inequality constraints optimally, a difficult problem in optimization. The technique presented rounds the corners of the thrust-time-curve, smoothly going from one constraint boundary to another. Also, the constraint boundaries are rounded at entry and exit.

One disadvantage in using spline-function interpolation in parameter optimization is that a perturbation in any one of the parameters modeling a control causes a perturbation in the spline over the entire range of the function definition. This, in turn, makes the gradient generation required by the Davidon-Fletcher-Powell function minimization algorithm a little more expensive compared to a sectionally linear interpolation.

Future research is recommended to determine the minimum number of data points required to model the thrust-time curve and still maintain integrity of the constraints and obtain maximum performance. A reduction in the number of parameters in this case could mean a large reduction in computation time and a less difficult problem to solve from the viewpoint of an iteration problem.

This method of parametrically defining a control function such as thrust by using spline-function interpolation can be applied to the modeling of vehicle attitude control functions such as pitch or angle of attack and bank angle, or any other control. The error function technique for satisfying inequality constraints can be used whenever the controls are approximated by a sequence of piecewise continuous linear segments or any other desireable parametric representation of the control as well.

References

[1] Johnson, I. L. and Kamm, J. L., "Performance Analysis of 049A/SRM Shuttle for Minimum GLOW," NASA-JSC Internal Note 72-FM-202, Sept. 1972, available through authors.

[2] Kamm, J. L. and Johnson, I. L., "Optimal Solid Rocket Motor Thrust Profile to Minimize 040A Shuttle GLOW," NASA-JSC Internal Note 72-FM-159, June 1972, available through authors.

[3] Kelley, H. J. and Denham, W. F., "Examination of Accelerated First-Order Methods for Aircraft Flight-Path Optimization," NASA CR-666681, Oct. 1968.

[4] Greville, T. N. E., "Spline Function, Interpolation, and Numerical Quadrature," Chap. 8, *Mathematical Methods for Digital Computers*, ed. by A. Ralston and H. S. Wilf, Vol. II, Wiley, New York, 1967.

[5] Fletcher, R. and Powell, M. J. D., "Rapidly Convergent Descent Method for Minimization," *Computer Journal*, Vol. 6, July 1963, pp. 163-168

[6] Kelly, H. J., Denham, W. F., Johnson, I. L., and Wheatley, P. O., "Accelerated Gradient Method for Parameter Optimization with Nonlinear Constraints," *Journal of the Astronautical Sciences*, Vol. XIII, July-Aug. 1966, pp. 166-169.

[7] Kamm, J. L. and Johnson, I. L., "Nonlinear Programming Approach for Optimizing Two-Stage Lifting Vehicle Ascent to Orbit," *Automatica*, Vol. 9, 1973, pp. 713-720.

[8] Johnson, I., "Error Function Method for Handling Inequality Constraints," NASA Internal Note 73-FM-114, July 1973, available through author.

[9] North American Rockwell Corp., "Data Sheet," 1973.

[10] Bryson, A. E., Denham, W. F., and Dreyfus, S. E. "Optimal Programming Problems with Inequality Constraints I: Necessary Conditions for Extremal Solutions, *AIAA Journal*, Vol. 1, Nov. 1963, pp. 2544-2550.

[11] Johnson, I. L., "Space Shuttle Vehicle Sizing with Maximum Dynamic Pressure Constraint Included," NASA Internal Note 72-FM-196, Aug. 1972, avilable through author.

[12] Lambert, C. H., "Solid Rockets," Engineering Design and Operation of Manned Spacecraft Seminar Series, Lecture 25, Spring, 1964, NASA.

[13] Johnson, I. L. and Kamm, J. L., "Near Optimal Shuttle Trajectories Using Accelerated Gradient Methods," presented at AAS/AIAA Astrodynamics Specialists Conference, Aug 17-19, 1971, Ft. Lauderdale, Fla.

[14] Johnson, I. L., "Optimal Rocket Thrust Profile Shaping Using Third-Degree Spline Function Interpolation," AIAA Paper 74-823, Anaheim, Calif., 1974.